The Flight Dynamics Risk Assessment of Artemis I

Eric C. Stewart,* Ivan Bertaska†
NASA, Marshall Space Flight Center, AL, 35812
Q. H. Zuo,‡ Scott Swatzel,§ Steve R. Hahn,¶ Thomas G. Howsman‖
Dynamic Concepts, Inc. Huntsville, AL, 35806

With launch vehicles and spacecraft, it is necessary to dynamically test the structure to validate structural models. These validated models are then used to determine a launch vehicle's control stability margin and the loads on the structure. While often a dedicated structural test article is used to correlate the integrated structure in preparation for the final analysis cycles, the Artemis I flight is using an approach where the components of the launch vehicle are dynamically tested and the component models validated. The fully integrated vehicle is not tested until a few months before launch, which limits the ability to fully correlate a model prior to launch. This paper introduces the Flight Dynamics Risk Assessment of the vehicle, which is the process being used to determine the adequacy of the vehicle structural model after the Integrated Modal Test. This work outlines the process of quickly tuning a model post-test then determining any control margin violations and increases in loads due to that tuned model.

I. Introduction

The Space Launch System (SLS), Orion Multi-Purpose Crew Vehicle (MPCV) and the Exploration Ground Systems (EGS) programs will come together for the Artemis I flight, where the SLS will launch an uncrewed Orion beyond the moon on a thre-week mission. SLS, Orion, and EGS have performed a series of element level and integrated vehicle static and modal tests culminating with the Integrated Modal Test (IMT) and Dynamic Rollout Test (DRT) which collectively serve as a building block approach to Artemis I finite element model validation.

Due to hardware availability constraints, some of this testing will occur towards the end of Artemis I vehicle's development and flight certification. The Artemis I Flight Readiness Analysis Cycle (FRAC) models will be correlated up through a subset of SLS Element and MPCV testing. Therefore, the Exploration Systems Development (ESD) and SLS Program will carry the risk into Artemis I flight that the integrated vehicle models do not accurately represent critical modes used in the development of design loads and vehicle control system parameters. The SLS Stages Element model will be correlated using only subelement static testing. The IMT will occur in the Vehicle Assembly Building (VAB) just prior to the DRT and the Wet Dress Rehearsal (WDR). Therefore, there will not be enough time between the end of the integrated test series and the first flight for the integrated vehicle FEM to be correlated with the IMT and DRT test data and then have updated loads and Guidance, Navigation, and Control (GN&C) assessments completed. If the nominal dynamic model does not sufficiently match the IMT data, then there is a risk of a 4-6 month launch delay for model correlation.

Towards the goal of mitigating this schedule risk and building adequate flight rationale that quantifies the technical risk, the Flight Dynamics Risk Assessment (FDRA) has been developed. The FDRA aims to

*Structural Dynamics Engineer, NASA MSFC; eric.c.stewart-1@nasa.gov
†Control Stability Lead, NASA MSFC; ivan.r.bertaska@nasa.gov
‡AIAA Associate Fellow, Senior Engineer/Scientist; kzuo@dynamic-concepts.com
§Engineer/Scientist; sswatzell@dynamic-concepts.com
¶AIAA Member, Senior Staff Engineer; shahn@dynamic-concepts.com
‖Senior Staff Engineer/Scientist; thowsman@dynamic-concepts.com

quantify impacts to vehicle design loads and stability margins due to the differences between the FRAC flex modes and those that are tuned to the results of the IMT.

A Best Modal Estimate (BME)[1] will be created to best model the IMT data. This model will not be fully correlated in accordance with NASA standards since the schedule does not allow for such an effort, but instead will be chosen out of a large family of models that will be generated through parametric dispersions of the FRAC integrated vehicle nominal test model, which is assembled from the Orion MPCV, SLS Elements, and EGS FRAC models. The family of models requires a voluminous amount of front end effort[2] using the FRAC models, but allows for a fast turnaround time (less than two weeks) for a tuned model once the test data is delivered. A single FRAC dispersed model will be chosen based on comparing the test data to the family of models through cross-orthogonality and frequency errors. From the BME, a series of flight models will then be created with the same parametric dispersions.

The FDRA is an accelerated loads and control stability assessment that will utilize the flight models generated from the BME process. This assessment will assess the effect of the updated models have on critical load indicators during critical load events, i.e., liftoff and max dynamic pressure, and control stability margins for all flight times.

For loads, the assessment will include quantifying the impact on load enclosure levels (probability of vehicle seeing the load) for the critical load indicators (CLI) as well as recommendations for mitigation options for any redline exceedances. For vehicle control stability, an assessment will be made for critical flight times on the impact the changes in the vehicle flex modes have on the open-loop stability margins at critical frequencies.

II. Best Model Estimate

The basis of the BME process is to disperse the material properties in the finite element model as a model tuning process. The model dispersions are perturbations of the nominal test configuration model. After a test, the mode shapes and mode frequencies of each dispersion are compared to the test data. The dispersion that best fits the test data is considered to be the BME of the test data.

A. Model Dispersions

Test model dispersions are used to quantify model uncertainty and to provide a best model estimate (BME). The method to produce these dispersions starts with the nominal test model, which is parsed to get the material properties from the NASTRAN bulk data files. Perturbation factors are then applied to material parameters in the model to either increase or decrease the parameter values off of their nominal values. Thousands of dispersions are created by applying these perturbation factors to the nominal model.

There are hundreds of material properties in the nominal model. If all of the material parameters are used to create the model dispersion, then little useful information can be pulled from this process since the individual material properties are small contributors to the mode frequencies and shapes. Therefore, the material properties to be used in the dispersions are a subset of the full set of material properties in the model. The subset of material properties used in the dispersions are those which have high sensitivity and by leveraging the SLS Elements' insight on important model parameters. To further reduce the number of parameters, material properties are often grouped together so that one perturbation factor increases or decreases all material properties in the group. These groups of parameters also increase the influence of one perturbation factor on the modes of the model, so more information can be pulled from the model with one parameter change.

B. Picking the Best Model Estimate

After the experimental mode shapes and frequencies are determined from the integrated modal test (IMT), they are then compared to the analytical mode shapes and frequencies for each of the dispersed models. The dispersed models' frequencies are compared to the test data frequencies as

$$g_1 = \sum_{i=1}^{f_i < TBD} W_i \frac{(f_i^{FEM} - f_i^{test})}{f_i^{test}} \tag{1}$$

Where select modes up to 7Hz are kept in the frequency error comparison since the PSMT and IMT sensor locations are determined using target modes to 7Hz. The term W_i is a weighting factor applied to indicate a test mode's relative importance to the vehicle structural dynamics in flight. This relative importance is determined by the three traceability methods. The test mode frequencies f^{test} are compared against the frequencies of the finite element model (FEM) f^{FEM}. Mode shape orthogonality is used to ensure that the test modes are compared against the analogous FEM modes. The modes associated with the dispersed models are also compared against the test mode shapes. The mode shape comparison uses the cross-orthogonality metric (XOR) as

$$XOR = \left(\phi^{FEM}\right)^T [M] \left(\phi^{test}\right) \tag{2}$$

ϕ^{test} is the matrix of test mode shape coefficients, ϕ^{FEM} is the matrix of analysis shape coefficients, and M is the Guyan-reduced FEM mass matrix reduced to the test sensor degrees of freedom. A perfect XOR matrix has ones on the diagonal. Therefore, the metric to measure the quality of all of the mode shapes is given as

$$g_2^{RSS} = \|[I]\,[W] - [XOR]\,[W]\|_{RSS}$$

Where RSS denotes the root-sum-square of the matrix diagonal. The RSS is beneficial because it only accounts for the on-diagonal and neglects the off-diagonal error. The RSS norm is also used in the commercial model tuning code Attune by ATA engineering.[3] After comparing all of the dispersions to the test data, one dispersion needs to be selected as the BME. However, some dispersions will compare well to the test frequencies while others will compare well to the mode shapes. This will generate a Pareto front of designs: a set of non-dominated optimal points. There is no set criteria for selecting the best dispersion, but it will selected by changing the weighting factors in the objective functions and comparing the dispersions against test data. The changing weighting factors will help determine which model is robust to different target modes sets.

C. Model Uncertainty

One of the goals of the IMT is calibration of the dynamic model, but this calibration can only be performed on the ground-configuration of that model. The accuracy of the flight configuration of the model, which is more important to meet the requirements, will still have some degree of uncertainty that will remain unaddressed, though, since no flight dynamic data will exist until launch. It is critical that an acceptable level of accuracy of the flight-configuration model be quantified. A technique has therefore been developed to quantify the probability that the pre-test flight dynamic model is an accurate representation of the dynamics of the SLS, i.e., if the model's fundamental frequency is within the requirements established by the vehicle controls flight software. If this probability of accuracy is below a given confidence value (established by agreement of the dynamics community), then the flight software would need to be redesigned. Since the true flight frequency is unknown until after the flight, it must be extrapolated from the IMT data in the ground configuration, the dynamic model of the IMT configuration, and the dynamic model of the flight configuration.

The technique to obtain this probability is defined as follows. First, a number of candidate SLS IMT modes that are similar to the critical flight mode are identified using a singular value decomposition technique to "map" the modes from the flight configuration to the ground configuration. The flight modes and ground modes are then compared via modal assurance criterial (MAC) and strain energy density. The details of this analysis are found in SLS-RPT-237-01. A Monte Carlo analysis using the same model parameter perturbations as used in the BME process is performed to give sample sets for each configuration. The statistical correlation between each candidate mode and the flight mode is calculated.

The perturbations for each configuration (IMT and Flight) are read into a Matlab script that performs a Quantile Linear Regression (QLR) analysis. This procedure generates linearly varying quantiles of the flight configuration natural frequency for any given value of the IMT configuration. The QLR process is similar to generating a conditional normal distribution for those values, without the Gaussian requirement. Once the modal test of the IMT is performed, the specific values of the test modal frequencies will be obtained, and the quantiles will be used to determine any additional flight risk by not changing the control design .

This technique was tested using the dynamic models, ground modal test data, and flight data from the Ares-IX launch vehicle. The parameter set and dispersions used are the same as in the original model validation efforts, as documented by Horta, et al.[4] A 500 sample Monte Carlo analysis was performed for the flight configuration at 90 seconds into flight to enable a comparison with flight measurement of the first bending mode at 93 seconds. The nominal model frequency for that configuration is 1.84 Hz, and the measured frequency is 1.95 Hz. The QLR results are shown in Figure 1, where each green line indicates a different probability level for different values of the independent variable, which is the frequency of the ground model. If a probability of 0.995 is desired that the flight model exceeds the requirement of 97% of

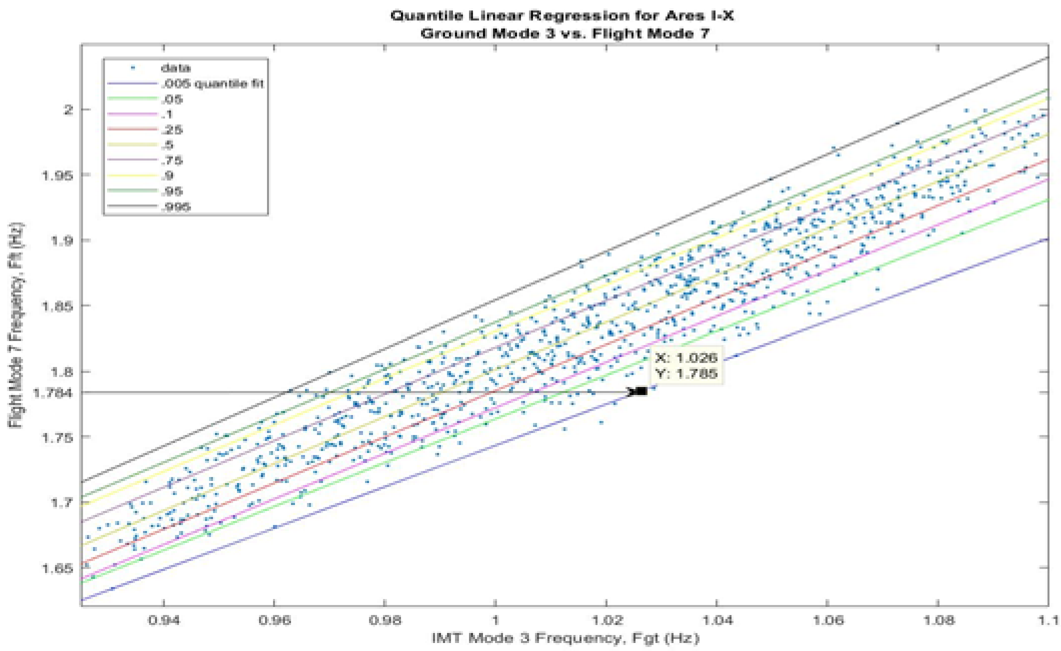

Figure 1. QLR on Ares I-X validation case

the nominal value, 1.78 Hz, then the intersection of this ordinate value with the .005 quantile (P(exceeding requirement)=1-.005=.995) yields a ground mode 3 frequency of 1.03 Hz, so any abscissa value above this would intersect with an even lower quantile, or higher probability of success. Since the actual ground test value was 1.06, it is clear that there is a nearly 100% chance that the flight met the criteria.

Since the technique performs adequately, it has been applied to the SLS model where 53 parameters have been incorporated into an SLS model that has been greatly reduced in computational size using the Augmented Modes Residual Vectors technique by Coppolino[5] , enabling a 2000 sample Monte Carlo run to be performed on both the ground and flight models. To illustrate this method, a case is shown here in which the random variables in the integrated vehicle are given a uniform distribution extending from -25% to +25% of the nominal values, and the Mobile Launcher random variables have a uniform distribution over +/-10%. The actual ranges of these distributions must be decided by the program. The liftoff mode of concern is mode 91 at 1.38Hz – the first pitch bending mode of the model. The IMT candidate modes are 12, 15, 16, and 19 at 1.22Hz, 1.45Hz, 1.46Hz, and 1.92Hz, respectively. Ground mode 12 is the best match to flight mode 91 from the SVD method and it has the best correlation from the Monte Carlo. For this case, there were a number of obvious outliers in the data; these resulted because the eigenvalue analysis of the specific sample set resulted in an entirely different mode. Since these are not realistic samples, they are eliminated from further calculations. The natural frequency of mode 91 using the nominal values of the parameters is 1.38 Hz, so the requirement will be set at .97*1.38 = 1.34 Hz. The sample sets of these two modes then were analyzed using the QLR script, and the resulting graph is shown in Figure 2, with a probability of success chosen for illustration to be 97.5%, corresponding to the .025 quantile. Two 95% confidence interval curves about the .025 quantile are also plotted, and the value of mode 12 from the IMT corresponding to the intersection of the lower bound curve with the 1.34 Hz flight frequency requirement is obtained from the graph to be 1.21 Hz. This value can be used to make the statement, therefore, that if mode 12 from the

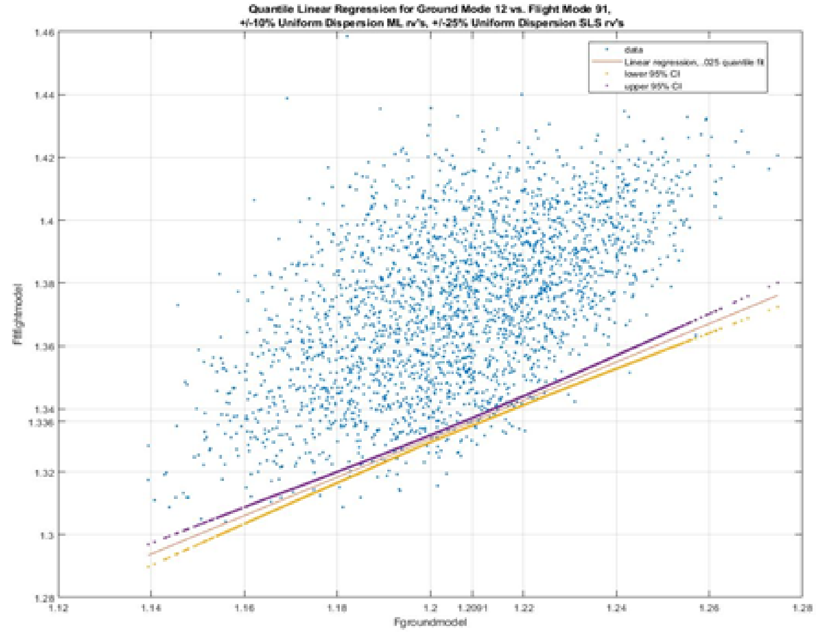

Figure 2. QLR with confidence limite on Artemis I dynamic model

IMT is greater than 1.21 hz, then the model has a 97.5% probability of being successful (i.e., the true value of flight frequency 91 is greater than 97% of the nominal model frequency 91), with a 95% confidence.

III. Control Stability Assessment

The BME flex model with the flight control system was assessed similarly to the way that EV41 conducts their typical control system analyses with flexible body dynamics. The BME flex model was processed and incorporated into the SLS control stability team's linearized frequency-domain control-system simulation, FRACTAL, the same way as any other officially delivered flex model. Since this design is completely gain stable (all modes display at least 12 dB of attenuation from 0dB), flex attenuation margin (AMf) is the driving parameter for passing the control system assessment. Providing sufficient flex attenuation is necessary to keep the flexible body dynamics from interfering with the control system response. With regards to the nominal flex model, the control system is designed to handle 12 dB of uncertainty (target 12 dB of AMf). This is reserved for 6 dB of uncertainty for damping variations and modal gain variations at each of the gimbals and sensors and an additional 6 dB of uncertainty for dynamics not modeled and unforeseen variations in plant parameters. For dispersions applied to the flex model – whether it be sub-element stiffness and mass dispersions from StE, or gain and frequency uncertainties applied by the controls team – the control system should always handle at least 6 dB of uncertainty (target 6 dB of AMf). Simply put, for a gain stable design, all flex modes should peak no greater than -12 dB for the nominal case, and -6 dB for any case that has flex uncertainties/dispersions applied.

For the Block 1 vehicle, the test-to-flight frequency variation is expected to be bounded by 9% for the first bending mode pair in pitch and yaw, and 20% for all other modes. Due to the gain stable design, the most stressing uncertainties tend to lie on the low bound of the range (i.e. 9% decrease on the first mode frequency). Bode stop-light charts were used to assess the BME flex model, both nominally and with the control-system-flex-model uncertainty bounds applied (9% down on first pitch/yaw modal frequency and 20% down on all other modal frequencies). Figure 3 shows a labeled template of the stop light charts that were used. The action taken is defined by the region that the modal peak lies in. The red over-hanging portion between 0 and -6 dB represents the flex filter roll off frequency, and is unique for each direction and each of the six ascent flight phases as defined by the flight control scheme.

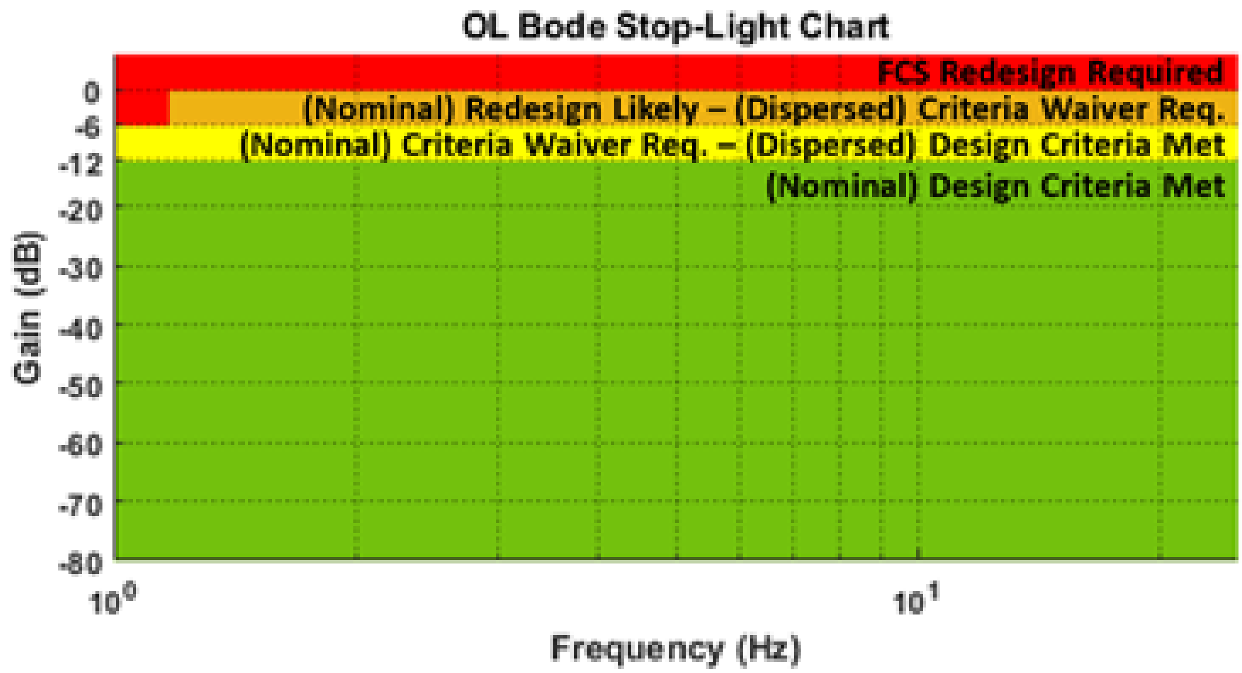

Figure 3. Labeled template of controls stoplight chart

Modal frequency adjustments are done by simply multiplying all modal frequencies by a single multiplier. To prevent having to identify and map each mode across every flight model, the uncertainty multipliers (0.91 for 9% on first mode, and 0.8 for 20% on other modes) were applied to each modal frequency in separate cases. For the 9% on first mode case, all modes in the bode-space are ignored except the first, and conversely for the 20% on all other modes case.

IV. Loads Analysis

The SLS IMT occurs in close proximity to the FRR and launch, precluding a traditional comprehensive model correlation process followed by a vehicle loads assessment. To address this issue a new approach of loads analysis, the Improved Base-Model Approximation (IBMA), has been developed for the FDRA. The IBMA approach uses a nominal (base) flight configuration model and a flight model projected from the tuned BME model that best matches the ground dynamic test data. The dynamic responses (acceleration and velocity) of the vehicle under the applied loads (buffet, gust, etc.) are computed using the BME. These dynamic responses of the tuned model are used to compute the dynamic (inertial and viscous) loads of the vehicle, which are then mapped onto the nominal model to recover the Critical Load Indicators of the SLS Elements and Orion MPCV. The element loads are recovered using the base model for the following reasons:

1. The elements have indicated a strong desire that the SLS Level II loads and modeling team not alter the Output Transformation Matrices (OTMs) associated with the base model. - The element modeling teams have built their models based on their knowledge of the local mass and stiffness distributions and internal load paths. - The latest element models available during the FDRA timeframe are the FRAC models, and these element models/OTMs will incorporate element-level testing.

2. Several of the element models incorporate proprietary modeling processes (e.g., hydro models) that are difficult to exactly duplicate.

3. The development of element OTMs can be a time-consuming process, which in turn puts additional pressure on the FDRA team.

A. Improved Base Model Approximation

Consider the dynamic response and primary structure loads of a vehicle. Let the mass, damping, and stiffness matrices of the nominal model of the vehicle be $M^{(N)}$, $C^{(N)}$, and $K^{(N)}$, respectively. The corresponding mass, damping, and stiffness matrices of the BME (tuned) model are designated by $M^{(B)}$, $C^{(B)}$, and $K^{(B)}$, respectively. The dynamic response of the BME model to the applied loads $F^{(B)}$ are given by the integration of the equations of motion

$$\left[M^{(B)}\right]]\left\{\ddot{u}^{(B)}\right\}+\left[C^{(B)}\right]]\left\{\dot{u}^{(B)}\right\}+\left[K^{(B)}\right]]\left\{u^{(B)}\right\}=F \tag{3}$$

With the solution of the dynamic response, the dynamic loads (inertial and viscous loads) on the BME model can be readily calculated:

$$\left\{F^{(B)}_{Inert}\right\}=-\left[M^{(B)}\right]]\left\{\ddot{u}^{(B)}\right\},\quad \left\{F^{(B)}_{Visc}\right\}=-\left[C^{(B)}\right]\left\{\dot{u}^{(B)}\right\} \tag{4}$$

Now consider the response of the nominal model. The equations of motion of the nominal model can be written as

$$\left\{u^{(N)}\right\}=\left[K^{(N)}\right]^{-1}\left(\left\{F^{(N)}\right\}-\left[M^{(N)}\right]\left\{\ddot{u}^{(N)}\right\}-\left[C^{(N)}\right]\left\{\dot{u}^{(N)}\right\}\right) \tag{5}$$

where $F^{(N)}$ is the externally applied loads on the nominal model. Equation 5 for the displacement of the nominal model can be thought of as the solution of balanced-load case at each instant in time. The dynamic loads (inertial and viscous loads) on the nominal model are found by mapping the dynamic loads on the BME model:

$$\begin{aligned}\left[M^{(N)}\right]\left\{\ddot{u}^{(N)}\right\}&=\left[T^{BN}\right]^T\left[M^{(B)}\right]\left\{\ddot{u}^{(B)}\right\}\\ \left[C^{(N)}\right]\left\{\dot{u}^{(N)}\right\}&=\left[T^{BN}\right]^T\left[C^{(B)}\right]\left\{\dot{u}^{(B)}\right\}\end{aligned} \tag{6}$$

The transformation matrix $\left[T^{BN}\right]$ used in Eq. 6 to map the dynamic loads associated with the BME to the loads on the nominal model was found by the Virtual Work Principle, which requires that equivalent virtual work be performed by the dynamic loads on the BME and nominal models when subjected to the same arbitrary virtual displacement field. The derivation of the transformation matrix $\left[T^{BN}\right]$ is given in Section B.

Once the dynamic response of the nominal model has been computed from Eqs. 7.3 and 7.4, the element loads can be recovered using the OTMs of the nominal model:

$$\{L\}=\left[LTMD^{(N)}\right]\left\{u^{(N)}\right\}+\left[LTMA^{(N)}\right]\left\{\ddot{u}^{(N)}\right\}+\left[LTMF^{(N)}\right]\left\{F^{(N)}\right\} \tag{7}$$

where $LTMD^{(N)}$, $LTMA^{(N)}$, and $LTMF^{(N)}$ are, respectively, the displacement, acceleration, and applied-force OTMs of the nominal model.

The steps involved in the IBMA process can be summarized as follows:

1. Compute the dynamic response by integrating the BME equations of motion, Eq. 3;
2. Apply the dynamic loads associated with the acceleration and velocity from the BME response to the nominal model as in Eq 4;
3. Algebraically solve for the displacement of the nominal model as quasi-static solution for each instant in time as in Eq 5;
4. Recover the structure loads by using the OTMs and the displacement and acceleration of the nominal model as in Eq. 7.

The element loads are recovered using the OTMs of the nominal model, which incorporates the element test results. The BME model, which is tuned to the vehicle's IMT results, is only used to compute the integrated system response and the dynamic (inertial and viscous) loads to be mapped onto the nominal model.

B. Mapping of Dynamic Loads

One of the key steps in the IBMA process is the mapping of the dynamic (inertial and viscous) loads from the BME model to the nominal model. This is accomplished by an application of the Virtual Work Principle as described in Craig and Kurdila.[6] Consider an arbitrary virtual displacement of the vehicle: the virtual work done by the dynamic force on the nominal model is the same as that on the BME model, as per the imposed constraint.

$$\left\{\delta u^{(B)}\right\}^T \left\{f^{(B)}_{Dyn}\right\} = \left\{\delta \bar{u}^{(N)}\right\}^T \left\{f^{(N)}_{Dyn}\right\} \tag{8}$$

Where $\left\{\delta u^{(B)}\right\}$ and $\left\{\delta \bar{u}^{(N)}\right\}$ are, respectively, the virtual displacements of the BME and the nominal model; $\left\{f^{(B)}_{Dyn}\right\}$ and $\left\{f^{(N)}_{Dyn}\right\}$ are the corresponding dynamic loads on the two models.

The virtual displacement vectors of the two models are related by requiring that the two models give the same virtual displacements of some physical grids that are common to both models:

$$\{\delta u_g\} = \left[D^{(B)}\right]\left\{\delta u^{(B)}\right\} = \left[D^{(N)}\right]\left\{\delta \bar{u}^{(N)}\right\} \tag{9}$$

In the equation $\{\delta u_g\}$ is the virtual displacement vector of the physical grids that are common to both models, $\left[D^{(B)}\right]$ and $\left[D^{(N)}\right]$ are, respectively, the displacement transformations for the BME and nominal models. It follows from Eq. 9 that

$$\left\{\delta u^{(B)}\right\} = \left[T^{BN}\right]\left\{\delta \bar{u}^{(N)}\right\} \tag{10}$$

where $\left[T^{BN}\right]$ is the transformation matrix relating the virtual displacement vectors of the two models

$$\left[T^{BN}\right] = \left[D^{(B)}\right]^{-1}\left[D^{(N)}\right] \tag{11}$$

It is noted that $\left[D^{(B)}\right]^{-1} = \left[\left[D^{(B)}\right]^T \left[D^{(B)}\right]\right]^{-1} \left[D^{(B)}\right]^T$is a pseudo-inverse of the matrix, as the number of independent rows in $\left[D^{(B)}\right]$, the displacement transformation matrix for the BME model, is typically less than the number of columns in $\left[D^{(B)}\right]$, which corresponds to the number of DOFs of the BME model. The substitution of Eq. 10 into Eq.8 yields

$$\left\{f^{(N)}_{Dyn}\right\} = \left[T^{BN}\right]^T \left\{f^{(B)}_{Dyn}\right\} \tag{12}$$

which is the mapping of the dynamic loads (inertial and viscous) from the BME model to the nominal model.

V. What's new in this paper

The SciTech version of this paper will include results from completed "dry runs" that show the capability and benefits of the Flight Dynamics Risk Assessement. These dry runs start by considering a randomly perturbed model as the "test data" then use a Best Model Estimate to estimate the loads and control stability of the "test data" in flight. The results show a good match to the "truth" model when perturbed "test data" model is projected into the flight configuration. To the authors' knowledge, no method similar to the FDRA analysis has been performed for any spacecraft or launch vehicle application until now.

References

[1]Stewart, E. C. and Hathcock, M. L., "Using Dispersed Modes During Model Correlation," *Proceedings of the 2017 AIAA SciTech Forum*, 2017.

[2]Stewart, E. C., Blelloch, P., and Coppolino, R. N., "Improving Accuracy of Structural Dynamic Modification with Augmented Modes Residual Vectors," *AIAA Science and Technology Forum and Exposition*, 2019.

[3]ATA Engineering, Inc., *Attune*, 2016.

[4]Horta, L., Reaves, M., Buehrle, R., Templeton, J., Lazor, D., Gaspar, J., Parks, R., and Bartolotta, P., "Finite Element-Model Calibaration for Ares I-X Flight Vehicle," 2011.

[5]Coppolino, R. N., *FEM Sensitivity Method for Uncertainty and Reconciliation Analyses*, Springer New York, New York, NY, 2011, pp. 375–382.

[6]Craig, R. R. and Kurdila, A. J., *Fundamentals of Structural Dynamics*, John Wiley and Sons, Inc., 2nd ed., 2006.